Periodica Polytechnica Civil Engineering, 68(1), pp. 248–259, 2024

Effects of Tire Crumb Rubber and Steel Fiber on Punching Shear Behavior of Two-way Alkali-activated Concrete Flat Slabs

Necip Altay Eren[1*], Abdulkadir Çevik[2]

[1] Department of Construction, Technical Science Vocational Schools, Gaziantep University, Üniversite Bulvarı 27310 Şehitkami, Gaziantep, Turkey
[2] Department of Civil Engineering, Gaziantep University, Üniversite Bulvarı 27310 Şehitkami, Gaziantep, Turkey
* Corresponding author, e-mail: altayeren@gantep.edu.tr

Received: 03 February 2023, Accepted: 15 September 2023, Published online: 04 October 2023

Abstract

As a result of the rapid increase in the demand for transportation vehicles recently, the accumulation of waste tires causes environmental problems. One of the methods that can contribute to the reduction of this environmental problem is the recycling of waste tires as a construction material in aggregate form. This research investigated the impacts of waste tire crumb rubber with/out steel fiber (SF) on the two-way punching-shear behavior alkali-activated concrete (AAC) flat slabs and performed center point load tests. In the study, one-type of SF and two kinds of scrap tire waste i.e., crumb rubber (CR) and tire particles, were used on the producing of rubberized AAC slabs obtained by 100% as binder made of ground-granulated blast furnace slag (GGBFS). Also, while both fine crumb rubber (FCR) and coarse crumb rubber (CCR) were used together in the AAC slabs, tire crumb rubber (TCR) was used alone at the same proportion. Additionally, the fine aggregate was substituted with 10% and 15% FCR and CCR, and coarse aggregate was substituted with TCR in the same proportions. Additionally, AAC slabs with recycled tire rubber (RTR) were produced as fibrous and non-fibrous using 1% by volume hook-end SF. In total, nine AAC slabs with sizes of 50 x 50 x 6 cm^3 were manufactured for the study. Experimental data showed that the inclusion of RTR only slightly reduced the punching shear strength of AAC slabs and the punching shear strength of the slabs increased when SF was added to the mixtures containing RTR.

Keywords

alkali-activated concrete, punching shear behavior, steel fiber, waste tire crumb rubber

1 Introduction

At the present, the storage of tires is also considered a major environmental danger, as used tire elimination areas reduce biodiversity owing to the toxical and solvable ingredients of tires [1]. Because of the fast increment in the demand for transportation owing to modern developments, the waste tire accumulation brings about ecological catastrophes. Additionally, the increase in the costs of collection, transportation and disposal of waste tires is also considered its prime issue. It is therefore vital to recycle trash tires for potential reuse in the construction sector as aggregates. The reuse of waste tires is becoming one of the ideal answers economically and for the ecosystem. Nevertheless, the tire rubber replacement rate should not be more than 20% to avoid a harmful impact on some mechanic features of the rubberized concrete [2]. One of the important problems for rubberized concrete is insufficient bonding between the concrete and the rubber matrix. Due to this insufficient bonding, premature cracking occurs in the concrete. For this reason, rubberized concrete is used in non-structural applications [3, 4]. Additionally, there are very few researhes in the literature on the punching shear performance of rubberized concrete. Thus, the number of studies on this subject should be increased.

After water, concrete is the material that is utilized the most globally [5]. To reduce CO_2 emissions, the construction industry must use eco-friendly products, so alkali-activated concrete is one of the alternative materials for the construction industry. (AAC), which is environmentally friendly concrete that could be obtained from rich aluminosilicate ingredients such fly ash, slag, metakaolin, and alkali solution [6–9]. Since OPC requires more energy and causes more environmental pollution, geopolymer or alkali active concrete is preferred instead of OPC concrete recently [10].

Cite this article as: Eren, N. A., Çevik A. "Effects of Tire Crumb Rubber and Steel Fiber on Punching Shear Behavior of Two-way Alkali-activated Concrete Flat Slabs", Periodica Polytechnica Civil Engineering, 68(1), pp. 248–259, 2024. https://doi.org/10.3311/PPci.21990

In practice, concrete flat slabs are extensively used in multi-storey car parks, some industrial structures, etc. In these systems, beamless columns directly support flat slabs, resulting in a substantial decrease in the height of the structure and an increase in the area used. However, in these systems, punching shear failure problem arises in slabs because of extreme stress condensation in slab-column joints. Owing to the brittle structure, such fractures are very unsafe and unwanted. Whenever a punching shear failure occurs, the structural strength significantly deceased, so the bond between the column and slab weakens and allocates, causing the entire structure to collapse [11].

In the literature, there are some techniques to decrease the effects of punching shear on column-slab connections and to raise the control of cracks that may occur. One of these techniques is to use SF in a matrix. As a result of previous research, it was found that the addition of fiber is beneficial in increasing the mechanical properties of concrete [12]. The use of SF in concrete increases the compressive force, and that enhancement modifies according to the SF content and sizes in the mix [13]. Besides, the results of the tests demostrated that the presence of SF in the concrete mixtures increased the punching shear strength of the slabs [11]. It was determined that the reason for these improvements was the capacity of the fibers to bridge the cracks, particularly after the concrete structure fractured. Additionally, the mainspring of using SF in AAC is to improve the post-cracking behavior of AAC [14]. Moreover, researchers found that the optimal amount of SF for economic reasons was 1% [15].

The recycled scrap tires were intended to be used as follows: specific concrete features such as ductility are improved by rubber particles or CR in concrete mixtures [16], toughness, or energy absorption [17], impact resistance [18], fatigue [19], and others [20]. Moreover, the use of crumb rubber instead of coarse or fine aggregate in concrete reduces the compressive strength, discrete tensile strength, modulus of elasticity and flexural strength of concrete, while increasing ductility and fracture toughness and impact strength of concrete, depending on the size and volume ratio of the crumb rubber [21]. Research on the punching shear strength of rubberized concrete slabs showed that as the quantity of rubber particles in the concrete, increases the punching shear strength of rubberized concrete slabs is decreased and the addition of up to 5% rubber compound causes a slight decrease in punching shear strength.

The primary purpose of this study is to investigate the punching shear strength of AAC flat slabs by using SF and RTR while improving existing study and conduce to the literature on AAC flat slabs. Additionally, this study conduces to the production of environment by turning industrial by-product materials such as GGBFS and RTR into useful materials and reducing CO_2 emissions due to the use of GGBFS as a binding material [10]. This study consists of two steps; in the first step, the effect of RTR alone on the punching shear strength and in the second step, the impacts of both RTR and SF together on the punching strength of slag-based AAC flat slabs were investigated. Additionally, one of the most major factors influencing the punching shear strength and fracture modes of rubberized AAC slabs with/out SF is considered the aspect ratio of the specimens. Additionally, the cracking patterns of these slabs were thoroughly explored, as well as the failure modes of rubberized AAC flat slabs with and without SF. In the literature, there are some analytic and empirical researhes exploring the effects of SF and RTR concrete slabs on the punching trends. Even tough some research have been investigated on the punching strength of AAC slabs in the literature, there are few research about the impact of RTR and SF on the punching strength capacity of AAC slabs.

2 Experimental program

2.1 Materials

AAC made from slag was bound together with the industrial byproduct material GGBFS, which has a specific surface area of 418 m^2/kg and a specific gravity of 2.70 g/cm^3. Table 1 represents the chemical compounds and physical features of the GGBFS material [22].

Table 1 The chemical compounds and physical properties of the GGBFS

Material	GGBFS (%)
CaO	34.12
SiO_2	36.4
Al_2O_3	11.39
Fe_2O_3	1.69
MgO	10.3
SO_3	0.49
K_2O	3.63
Na_2O	0.35
Loss of Ignition (%)	1.64
Specific Gravity (g/cm^3)	2.76
Blain Fineness (m^2/kg)	4.18

The crushed limestone coarse and fine aggregates were obtained from the original source used to produce AAC mixtures. The physical characteristics and the sieve analysis of aggregates are presented in Table 2 and Fig. 1 [23, 24].

In this study, the RTR materials were substituted with aggregates. 10% and 15% of coarse and fine aggregates were used in place of TCR and CR, respectively, as shown Figs. 2(a), 2(b) and 2(c). Additionally, during the production of AAC flat slabs, CCR and FCR were used equally in mixtures of both 5% and 7.5% in two different ratios instead of aggregate, respectively. The physical features and sieving analysis of RTR were displayed in Table 3.

Table 2 The physical characteristic of aggregates [24]

Materials	Fine Aggregate	Coarse Aggregate
Fineness Modulus	2.57	5.66
Specific Gravity	2.45	2.72
Water Absorption	1.5	2.4

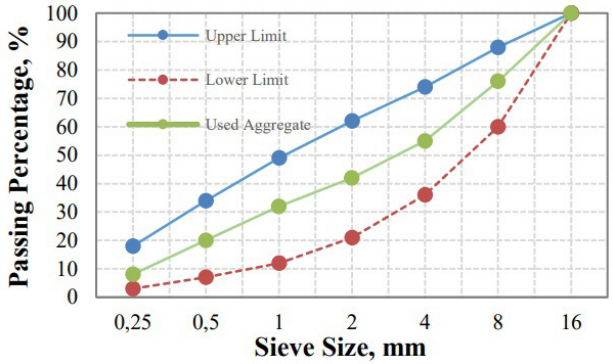

Fig. 1 The sieve analysis of aggregates [23]

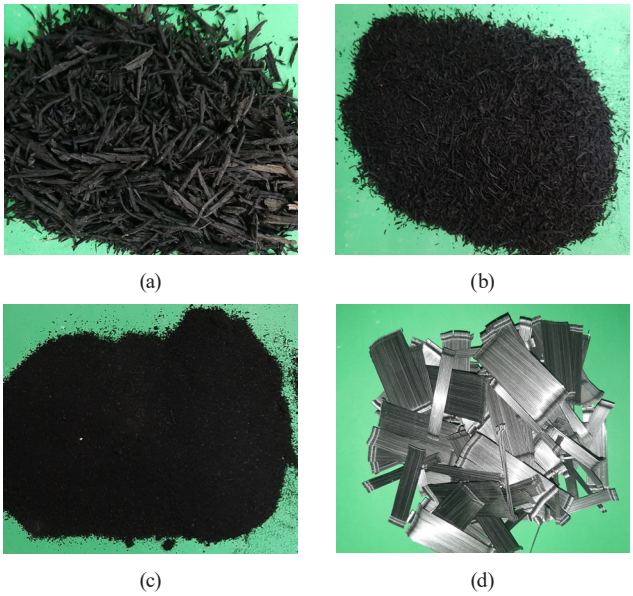

Fig. 2 Tire, coarse, fine crumb rubbers and Steel Fiber used in the AAC slab specimens, (a) Tire crumb rubber (TCR), (b) Coarse crumb rubber (CCR)

Table 3 The Sieve Analysis and Physical characteristics of RTR [24]

Sieve Size(mm)	CCR	FCR	TCR
16	12.2	11.1	5.3
8	21.8	47.4	9.6
4	33.5	86.3	24.6
2	81.7	100	53.8
1	100	100	89.6
0.5	100	100	100
0.25	100	100	100
Fineness Modules	2.23	1.97	3.88
Specific Gravity	0.83	0.48	1.02
Absorption (%)	2.2	1.8	2.9

A mixture of NaOH solution and Na_2SiO_3 solution at room temperature was used as the alkali activator. This alkaline activator was made available 24 hours before being used in the GPC mix. The Na_2SiO_3 solution is commercially available in component ratio (SiO_2: 29.4, water: 55.9% and Na_2O: 13.7% by mass). The NaOH was available in solid form as pellets [22]. These solid pellets were dissolved in water to obtain NaOH solution of the necessary concentration [25]. The NaOH had 97–98% purity. In this research, the molarity of NaOH was designed to be 12M (molar) because, the best performance of AAC is achieved in 12M NaOH solu-tion according to many researchers [26]. According to the prior research, the Na_2SiO_3/NaOH ratio should be between 1.5 and 2.5 for economical causes [27]. Thus, this ratio was chosen as 2.5 in the study. Moreover, in this research, one type of Kemerix 30/40 hooked-end SF was added to the rubberized AAC slabs at 1% to investigate their punching shear performance, as shown Fig. 2(d). Table 4 shows the aspect ratio and geometrical characteristics of the SF.

2.2 Mix-design

Nine AAC mixes in all were created for this investigation and produced in two series. One of them was the mixtures including 10% and 15% RTR only, the other was the mixtures containing 10% and 15% RTR and 1% hooked-end SF. In this study, the individual RTR effect and the combined RTR and SF effect were examined in relation to the punching shear behavior of AAC slabs. A fixed 100% GGBFS was utilized as a binder in all ACC mixtures.

Table 4 The aspect ratio and geometric characteristics of SF

Designation of Steel Fiber	Diameter (mm)	Length (mm)	Aspect Ratio
SF	0.75	30	40

In all mixtures, the total amount of binder and SF were used as 500 kg/m^3 and a volume fraction of 1%, respectively. The quantity of each ingredient of rubberized fibrous AAC mix for 1 m^3 was represented in Table 5 [28].

The punching shear performance of AAC slabs is mostly influenced by binder quantity and kind, alkali activator quantity and proportion, aggregates, maximal particle dimension (Dmax), volume proportion, and SF aspect ratio. Firstly, dry mix for 2.5 minutes with aggregates and binder was done to obtain AAC mixes. The polycarboxylate-based Master Glenium-RMC-303 superplasticizer, more water and within 1 minute, alkaline activator was added to the dry mix, and it was then agitated for a further 2 prepared and cast 50 cm × 50 cm × 6 cm slabs for testing the punching shear strength tests, as shown in Fig. 3. The rubberized AAC slabs were covered with plastic as soon as the casting process was complete to prevent the evaporation of the alkaline activator solution. The samples were demolded 24 hours after casting minutes. After then, the mixture was blended for an additional 3 minutes to confirm that the rubberized AAC mixes were monotonous. Rubberized AAC slabs were and maintained in the lap room at 23±2 °C from the rubberized AAC samples until day 28. The punching shear tests of the AAC slabs were carried out at the same time. Also, during all punching shear experiments, the force was increased nonstop until all slabs collapsed. As indicated in Fig. 3, the testing was done using a BESMAK-Dual Frame Compression-Flexural Test Machine (300 kN capacity), which was made in compliance with EN 14651, TS EN 12390-5, EN 1339, EN 1343-44, and ASTM C-78 standards. Additionally, these slabs were loaded at 0.4 millimeters per minute displacement speed. As shown in Fig. 3, a particular steel structure support with eight immobilized steel hemispheres, specially manufactured for punching shear tests of AAC slabs, was used. The half steel balls were allowed to rotate freely so that there was no significant backlash to the slabs. The half steel balls were allowed to spin freely around themselves so that there was no significant counteraction to the slabs [28]. Furthermore, the surfaces of the half balls were manufactured in such a way that they did not harm the AAC slabs due to the singular stresses in the contact area. As shown in the following Fig. 3, these balls were positioned evenly apart on the steel structure, with a center angle of 45° and a diameter of 40 cm.

Table 5 Component of rubberized AAC slabs [28]

Mixture	GGBFS	SF	FCR	CCR	TCR	Fine Agg.	Coarse Agg.	Na_2SO_3 +NaOH	Molarity	SP
	kg/m^3	kg/m^3	kg/m^3	kg/m^3	kg/m^3	kg/m^3	kg/m^3	kg/m^3		%
GS	500	0	0	0	0	860.07	738.12	250	12	7
GS-5.0FCR-5.0CCR	500	0	7.95	10.65	0	780.44	738.12	250	12	7
GS-7.5FCR-7.5CCR	500	0	11.9	15.98	0	700.80	738.12	250	12	7
GS-10TCR	500	0	0	0	30.9	621.16	738.12	250	12	7
GS-15TCR	500	0	0	0	46.36	541.53	738.12	250	12	7
GS-1.0SF-5.0FCR-5.0CCR	500	78.4	7.95	10.65	0	779.00	736.76	250	12	7
GS-1.0SF-7.5FCR-7.5CCR	500	78.4	11.9	15.98	0	699.51	736.76	250	12	7
GS-1.0SF-10TCR	500	78.4	0	0	30.9	620.02	736.76	250	12	7
GS-1.0SF-15TCR	500	78.4	0	0	46.36	540.53	736.76	250	12	7

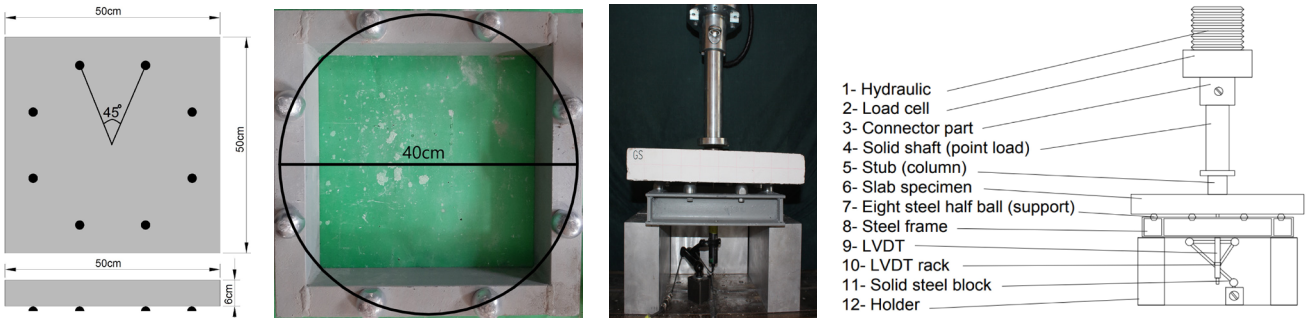

(a) (b) (c) (d)

Fig. 3 Punching shear test setup detail [23]; (a) Circumferential load distribution, (b) Special Steel Support, (c) Test setup on test machine, (d) Diagram representation of punching shear test setup

3 Results and discussions

3.1 Compressive strength

According to the ASTM C39 standard, compressive strength tests were performed 28 days after the casting of the AAC slabs to determine the compressive strength values using 3 pieces of 10 cm × 10 cm × 10 cm cubic specimens the findings of these specimens' tests were given in Table 6. These results indicated that the reduction trend was obtained with the addition of RTR. Additionally, the results clearly demonstrated that the compressive strength of the AAC specimens decreased as the amount and size of CR increased. Meanwhile, the addition of SF to the rubberized AAC positively affected the compressive strength results and improved these results. But these compressive strength values are lower than those of GS. The results showed that in rubberized samples, the compressive strength increased as the rubber ratio and size increased in the fibrous samples.

Reductions of these compressive strengths were achieved as 21.97% for GS-5.0FCR-5.0CCR, 33.09% for GS-7.5FCR-7.5CCR, 26.2% for GS-10TCR and 35.79% for GS-15TCR. Additionally, the declines in the compressive strength of fibrous samples were found as 7.2% for GS-1.0SF-5.0FCR-5.0CCR, 15.85% for GS-1.0SF-7.5FCR-7.5CCR, 10.19% for GS-1.0SF-10TCR and 17.66% for GS-1.0SF-15TCR. Meanwhile, these results demonstrated that the AAC slabs' compressive strength was greatly boosted by the addition of SF, and the GS sample with SF had the maximum compressive strength value. Since the stiffness of rubber is lower than that of tiny aggregate particles in many experiments, the reduction in compressive strength of the rubberized AAC specimens was attributed to the CR particles serving as voids and the porous nature of the piece rubber [29]. Other factors include flaws in the vicinity of the aggregate and a change in the elastic modulus of the rubber particles and cement paste [30]. Additionally, as the amount of CR increased in the AAC samples, the whole pore volume of these samples increased. Thus, the compressive strength results were adversely impacted. The compressive strength of SF reinforced concrete containing small amount CR aggregate particles slightly reduce the compared to plain concrete [31]. Similar results were obtained by previous studies [32].

3.2 The punching shear behavior under static loading

In this study, mid-deflection loading at a speed of 0.02 mm/min was used for all punching shear tests on 50 cm × 50 cm × 6 cm AAC slabs. A linear variable displacement transducer (LVDT) positioned in the middle of the specimens was employed during all experiments to gauge the slab center's mid-displacement. In addition, a steel plate with a diameter of 7 cm and a thickness of 1 cm hardened steel circle plate was used to as a column during the tests to transfer the punching loads from the hydraulic jack via the load cell to slabs. Additionally, the AAC slabs' force vs. deflection curves from the punching shear tests were shown in Fig. 4. Additionally, Table 6 displays the greatest force values of all tested specimens. All AAC slabs' pre-peak regions in punching tests showed a linear trend until the first fracture, and the post-peak regions showed strain softening. The impacts of RTR on the force vs. mid-deflection of AAC slabs with/out SF are shownn in Fig. 4(a) and 4(b). According to the results, rubberized AAC slabs without SF had a lower punching shear strength than GS. Because the stiffness of aggregate substitute with RTR was more than RTR. So, it caused an increase of pore volume in the rubberised AAC slabs. But RTR caused the ductility of rubberised AAC slabs to increase. Additionally, the inclusion of SF increased the punching shear strength of the rubberized AAC slabs.

Table 6 The punching shear test results of AAC slabs

Slab Samples	Compressive Strength (MPa)	Max. Disp. (mm)	Ultimate Punching Force in Experiments (kN)	Ultimate Punching Force from Regression Pattern (kN)	Exp/RP
GS	51.80(±0.93)	3.78	17.15	17.1502	0.99998
GS-5.0FCR-5.0CCR	40.42(±0.82)	14.22	15.42	15.4642	0.99714
GS-7.5FCR-7.5CCR	34.66(±0.78)	9.48	12.62	12.6177	1.00018
GS-10TCR	38.23(±0.91)	5.82	16.63	16.5715	1.00353
GS-15TCR	33.26(±0.85)	22.56	13.26	13.2883	0.99787
GS-1.0SF-5.0FCR-5.0CCR	48.07(±0.95)	43.82	18.04	17.9571	1.00461
GS-1.0SF-7.5FCR-7.5CCR	43.59(±0.88)	45.38	19.02	19.2533	0.98788
GS-1.0SF-10TCR	46.52(±0.84)	33.38	18.75	18.8052	0.99706
GS-1.0SF-15TCR	42.65(±0.72)	50.75	20.54	20.5191	1.00101

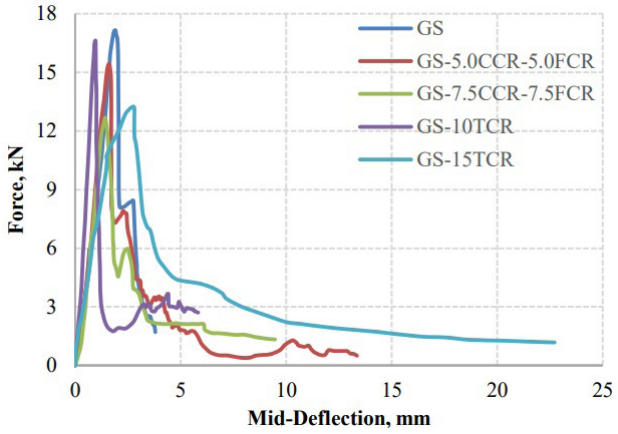

(a)

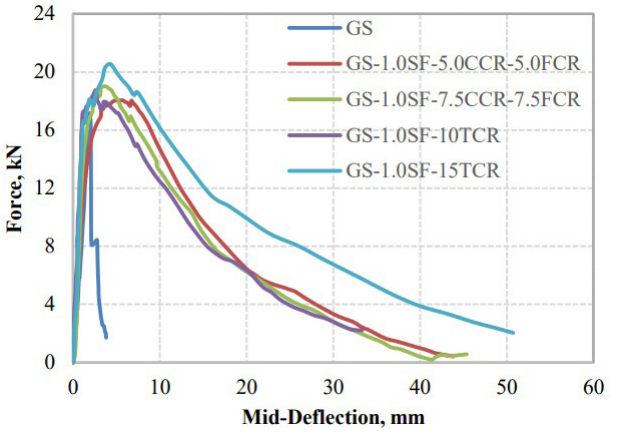

(b)

Fig. 4 The AAC slabs' punching shear test results; (a) Effects of RTR on AAC slabs, (b) Effect of SF on rubberised AAC slabs

Moreover, it was claimed that the rubberized AAC specimens with SF had a higher punching shear strength than the rubberized AAC slabs without SF. Also, the test results showed that slabs containing larger RTR particles had more punching shear strength than slabs containing smaller RTR particles. Parallel results were acquired for rubberized concrete slabs in former research [33]. Also, results showed that SF made the rubberized slabs' punching shear strength higher. Because, RTR particles improved ductility, while the presence of SF increased bonding under cracks and ductility. Furthermore, the size and content of RTR influenced on the fibrous AAC slabs' punching shear resistance. The punching shear strength of fibrous AAC slabs increased as the size and content of RTR increased. It was found that the use of RTR was particularly effective for post-peak performance, as shown in Fig. 3(a). According to the results, while GS-1.0SF-15TCR had the highest punching shear strength, the lowest punching shear strength was obtained from GS-15TCR. It means that the rising in the strength can be depends on the bond among the SF and matrix. It means that the rising in the strength can be depended on the adherence between the matrix and the SF. Moreover, because of its further elastic modulus, SF facilitate stress distribution, thereby restricting the formation of tension cracks and increasing punching performances. Another reason for the increase in punching shear strength in AAC slabs containing SF can be the increasing in the bond strength owing to the crack-stopping ability of SF. Further, the amount and type of binder, the amount and proportion of alkali-activator, aggregates, maximum grain size (Dmax), size and content of RTR, percentage of SF, and the dimension of the slabs were the main factors influencing the punching shear strength of AAC slabs.

According to earlier studies, the SF had a positive impact on the bond strength [34], fracture modes, and punching shear strength [35]. Also, studies revealed that as the CR ratio increased, the strength of the concrete dropped. The decrease in concrete strength is based on the fact that the hardness and rubber density is less than that of fine aggregates. Compared to rubber particles and cement paste, fine aggregates and cement paste have a larger interface transition area [36]. It was discovered that the shear strength of rubberized concrete beams was adversely affected by the addition of CR as a fractional replacement for natural aggregates [37]. In addition, it was presented that the using of CR in matris improved the cracking behavior, ductility and toughness of these structural elements [38]. The research results showed that rubberized AAC slabs containing SF possessed greater toughness and were more ductile than just rubberized AAC slabs, as shown in Fig. 4(a) and 4(b). Meanwhile, the force vs. mid-deflection graphs for rubberized with/out SF slabs were obtained to be parallel trends. Consequently, it was obviously observed RTR reduced the punching shear strength of the slabs, but it improved the toughness and ductility. In addition, the adding of SF to the rubberised slabs caused the improvement of ductility, toughness, and punching shear strength.

The fracture crack width obtained from each AAC slab in the study. Since SF distributes tensile loads along the fracture, it may result in a narrowing of the crack. Therefore, SF enchanced the punching shear strength, load carrying capacity, ductility, and post-crack of slabs. Additionally, if the post-cracking load kept getting better, it increased the width of existing cracks and led to new cracks forming. Moreover, according to the test results, RTR and SF enhanced the slabs' post-cracking and

ductility behavior, however RTR did not raise the punching shear load. Almost all slabs were totally failure, just for two slabs, GS-1.0SF-5.0FCR-5.0CCR and GS-1.0SF-7.5FCR-7.5CCR, the ultimate crack width was observed, 35mm and 15mm respectively. The reasons for these improvements or reductions were related to kinds, volume fraction and quantity of RTR also SF content. They were also impacted by the homogeneous distribution of RTR and SF in the matrix. Punching shear loads dropped as the size and amount of RTR in the mix increased, but the slabs' post-cracking and ductility behavior improved, as indicated in Fig. 4(a). Also, they were further enhanced by the presence of SF in the rubberized ones than just AAC slabs with RTR, as represented in Fig. 4(b).

3.3 Scanning electron microscopy (SEM) analysis

SEM photographs of rubberized AAC slabs with and without SF were given in Fig. 5. The SEM findings demonstrated that the microstructure of the SF-enhanced AAC samples was more uniform and denser. Also, gaps and angular slag grains were hardly seen. Additionally, the results showed that well-dispersed matrices with more reacted slag particles have a denser, more uniform and less porous microstructure, and therefore these samples have better mechanical properties. However, due to water evaporation, self-drying [39], and reaction product shrinkage [40], bigger interconnecting macrocracks were seen in the microstructure and shrinkage of reaction products. Therefore, the bond between the rubber pieces and the matrix weakened and the mechanical strength of the sample decreased.

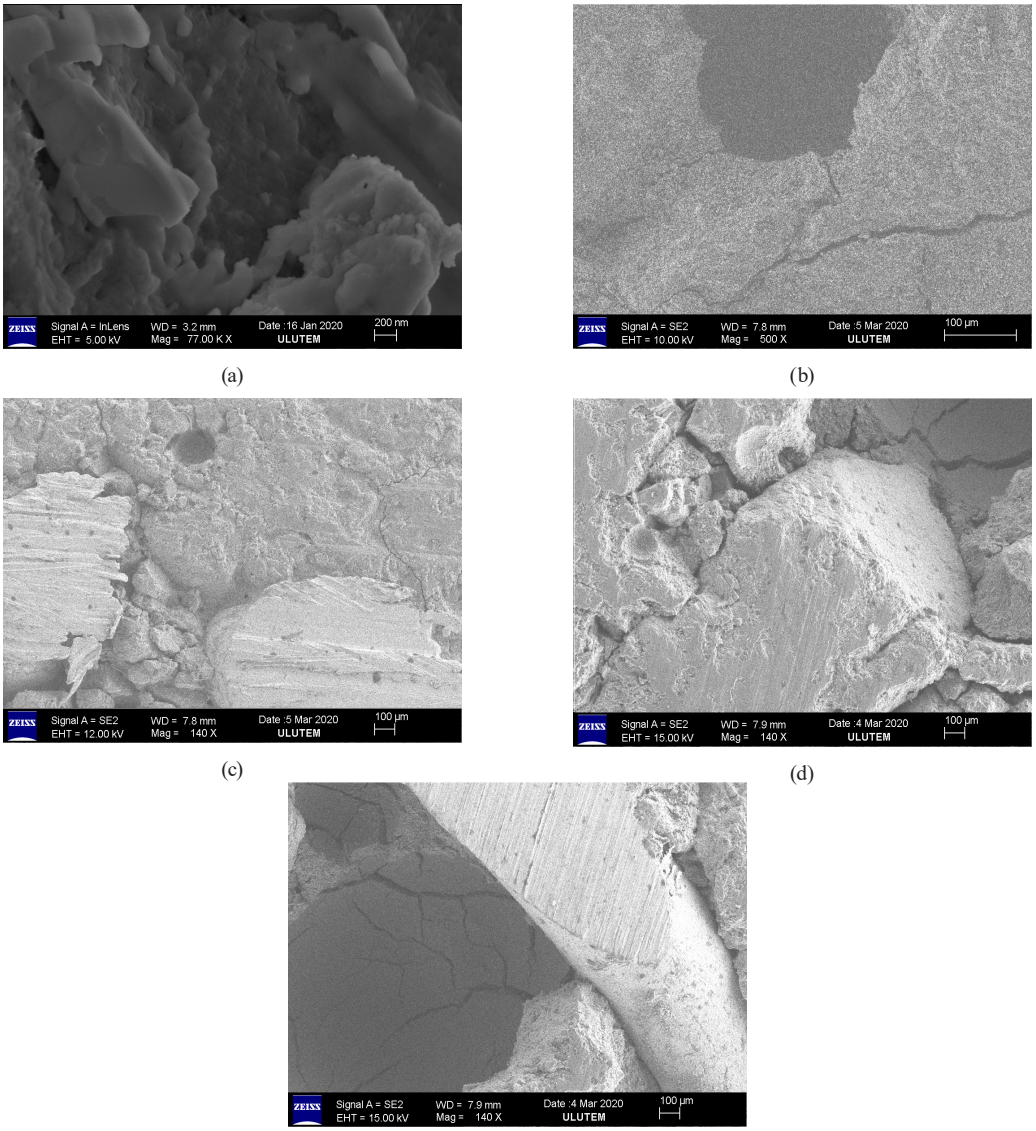

Fig. 5 SEM images of rubberized GC slabs with/out SF; (a) GS, (b) GS-7.5FCR-7.5CCR, (c) GS-1.0SF-7.5FCR-7.5CCR, (d) GS-15TCR, (e) GS-1.0SF-10TCR

3.4 Failure modes of the AAC slabs under punching

The rubberized materials' cracking patterns AAC slabs under center punching load were shown in Fig. 6. Moreover, Fig. 6(a) represents prior to failure and Fig. 6(b) afterward failure. The fracture pattern photos of the rubberized AAC slabs fibrous and non-fibrous were given. The test results showed that RTR and SF influence the crack patterns of ACC slabs. Flexure type cracks and flexure fractures were obtained for all slabs, as there were no conventional reinforced steel bars. One or more large main and microcracks were observed in the tension zone for the slabs, as shown in Fig. 6(b). Also, these cracks formed in the maximum moment zone. These cracks appeared from the center to the corners and edges. Also, they showed in Fig. 6(c) for after the front face fracture and Fig. 6(d) for after the back face fracture. For rubberized

AAC slabs only, the crack propagation of GS-5.0FCR-5.0CCR and GS-10TCR was similar, and the crack propagation of GS-7.5FCR-7.5CCR and GS-15TCR, as shown in Fig. 5(d). When cracks reach the rubber particles, due to the elastic features and low elasticity modulus of the rubber, the rubber grains extend and sustain some of the applied force, causing in an increasing of the fracture surface area. Moreover, for the fibrous rubberized slabs, the crack propagations are parallel to each other. Due to the sufficient bridging of cracks, hook-end SF continue preventing the more advanced levels of crack propagation till the structural member failure.

3.5 Regression pattern

Due to this experimental study; a numerical pattern was developed to determine the punching shear force for the rubberized AAC slabs used in the study. For this reason, the following numerical pattern was generated by using the compressive strength, steel fiber ratio, sizes of the AAC slab element, FCR, CCR and TCR ratios as variables. This pattern is produced handling the principle of least squares and is shown below as a pattern with a correlation coefficient of 0.999429. Additionally, the data obtained from the pattern are shown in Table 6. It was figured out that the pattern was changed by almost 2%. According to the data obtained from the pattern, it was observed that acceptable results were obtained from the produced numerical pattern. Notations are taken as:

$$\begin{aligned} V_{PL} &= 10.786xSF + 9.7489xf_{ck} + 6.9276xCCR \\ &+0.09712xTCRxf_{ck} - 190.598 - 0.20603xCCRxf_{ck} \\ &-0.11078xf_{ck}^2 - 0.002789xTCRxf_{ck}^2 \end{aligned} \quad (1)$$

Where

V_{PL}: Ultimate punching shear force in kN
SF: Ratio of SF fibers
FCR: Ratio of fine crumb rubber
CCR: Ratio of coarse crumb rubber
TCR: Ratio of tire crumb rubber
f_{ck}: Compressive strength at day 28 in Mpa

4 Conclusions

In the scope of the research, the punching shear strength of RTR and/or SF slag-based AAC slabs were investigated. Moreover, evaluation of the effects of SF and RTR on punching shear. Additionally, the effects of RTR size and quantity on the punching shear and failure modes of AAC slabs were researched. The following conclusions can be derived from the data acquired based on the outcomes of the tests conducted here:

The results showed that the presence of RTR has a negative impact on compressive strength. According to the results, as the size and content of RTR increased, the compressive strength of non-fibrous AAC slabs decreased. This reducing in compressive strength can be expressed by the weakness of the cohesion and poor bond between the rubber pieces and the AAC matrix, as well as the increase of voids that may have formed due to the FCR particles. Moreover, the existence of SF improved the compressive strength of rubberized AAC slabs, but they were less than the compressive strength of GS. Because these slabs included the RTR. Additionally, as the size and volume of RTR increased in the fibrous rubberized AAC specimens, the compressive strength of AAC decreased. Furthermore, the maximum and minimum compressive strengties were obtained from GS and GS-15TCR, respectively.

The results showed that both RTR and SF also influenced the punching shear strength. The size and amount of RTR in the AAC slabs impacted the punching shear strength. As the size and amount of RTR increased, the punching shear strength decreased. RTR due to their elastic features and poor elasticity modulus caused the pore volume of AAC slabs. While they decreased the compressive strength, the punching shear strengties were improved. Moreover, sametime RTR enhanced the ductility. Additionally, the addition of SF in the rubberized AAC slabs increased both the compressive and punching shear strengthes. This was because, the hook-end SF provided adequate bridging of cracks and this effect persisted until fracture.

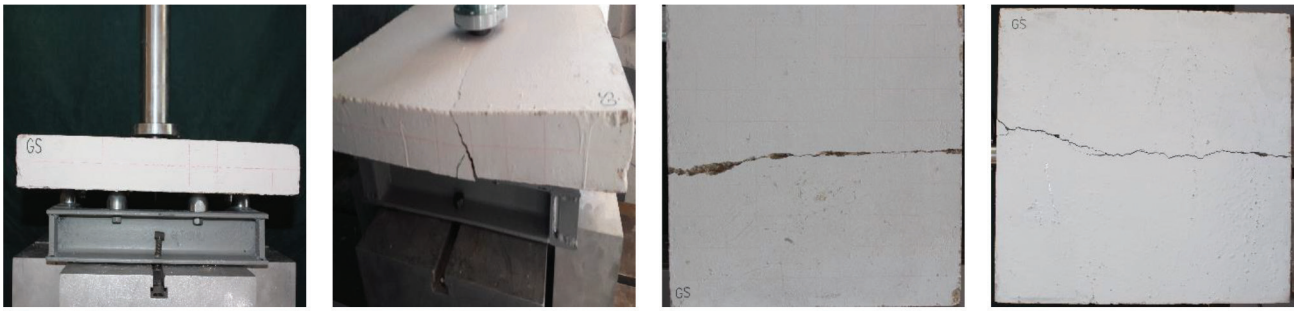

GS

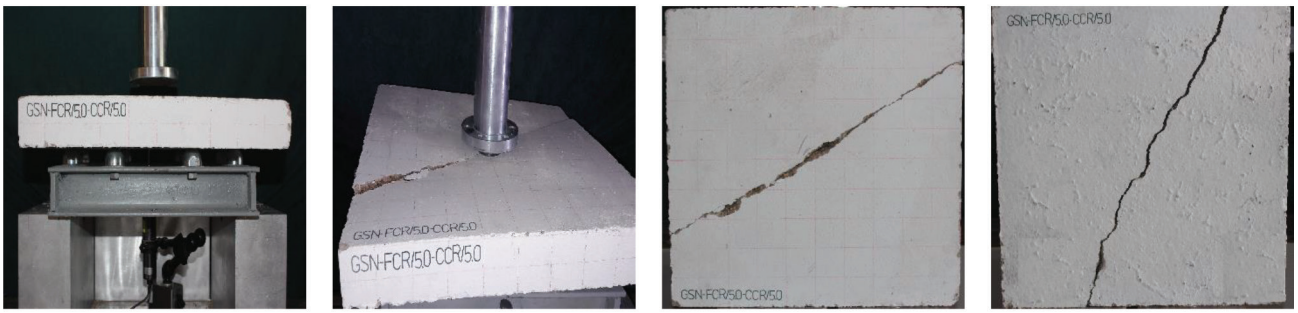

GS-5.0FCR-5.0CCR

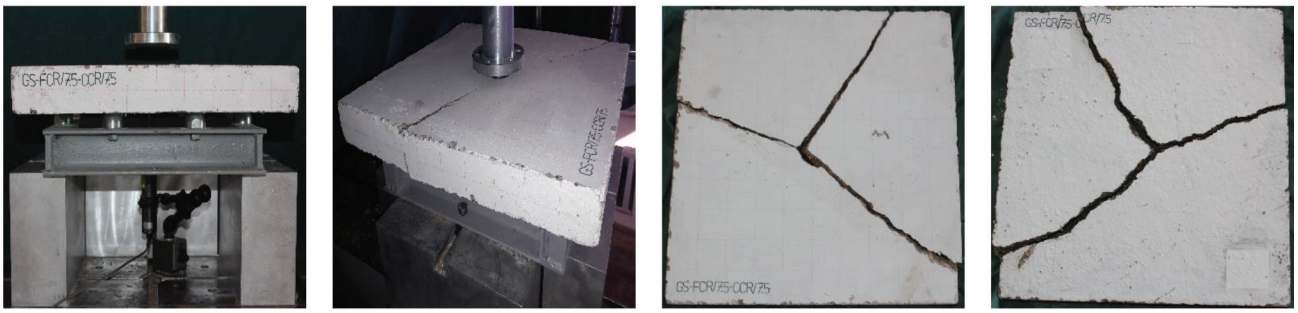

GS-7.5FCR-7.5CCR

GS-10TCR

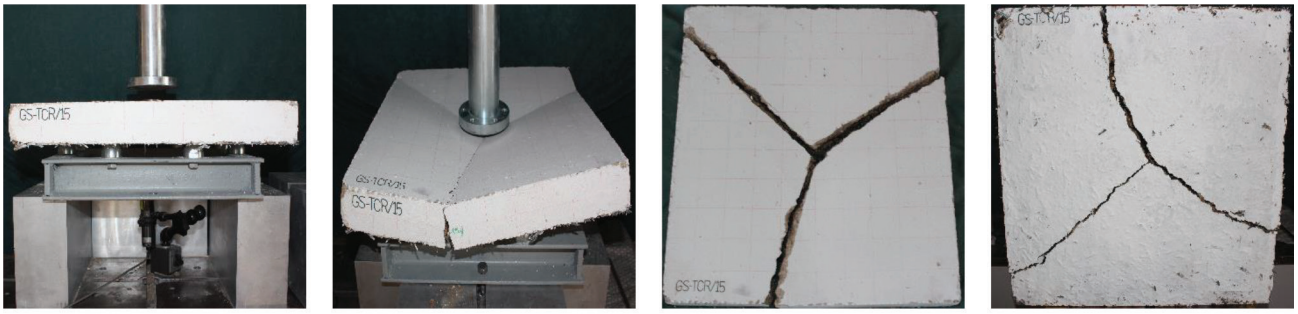

GS-15TCR

(a) (b) (c) (d)

Fig. 6 Failure modes of AAC slabs after punching shear tests; (a) Before failure, (b) After failure, (c) Front surface after failure, (d) Back surface after failure

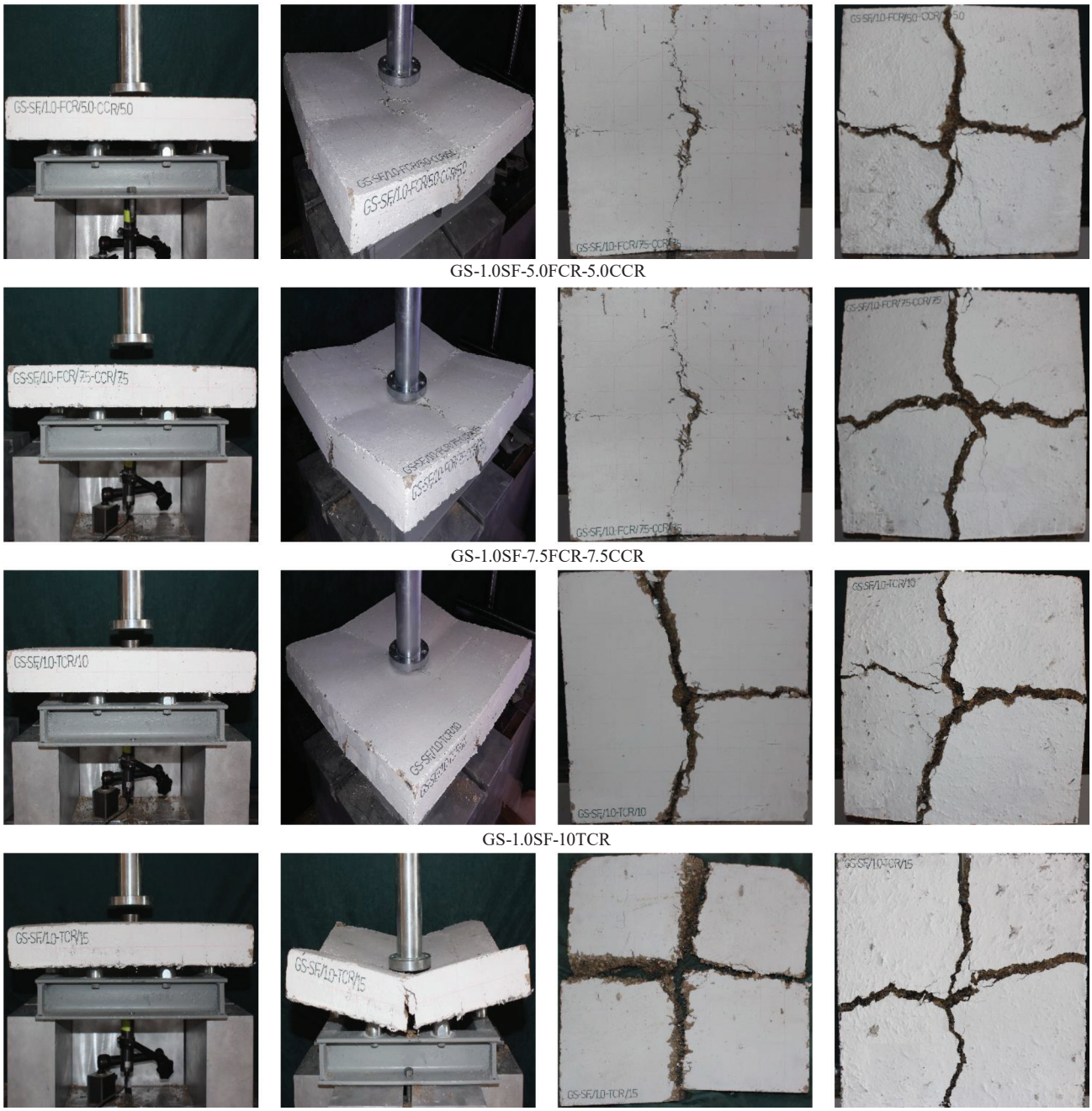

Fig. 6 Failure modes of AAC slabs after punching shear tests; (a) Before failure, (b) After failure, (c) Front surface after failure, (d) Back surface after failure

References

[1] Pacheco-Torgal, F., Ding, Y., Jalali, S. "Properties and durability of concrete containing polymeric wastes (tire rubber and polyethylene terephthalate bottles): An overview", Construction and Building Materials, 30, pp. 714–724, 2012. https://doi.org/10.1016/j.conbuildmat.2011.11.047

[2] Gholampour, A., Ozbakkaloglu, T., Hassanli, R. "Behavior of rubberized concrete under active confinement", Construction and Building Materials, 138, pp. 372–382, 2017. https://doi.org/10.1016/j.conbuildmat.2017.01.105

[3] Chan, C. W., Yu, T., Zhang, S. S., Xu, Q. F. "Compressive behaviour of FRP-confined rubber concrete", Construction and Building Materials, 211, pp. 416–426, 2019. https://doi.org/10.1016/j.conbuildmat.2019.03.211

[4] Ganjian, E., Khorami, M., Maghsoudi, A. A. "Scrap-tire-rubber replacement for aggregate and filler in concrete", Construction and Building Materials, 23(5), pp. 1828–1836, 2009. https://doi.org/10.1016/j.conbuildmat.2008.09.020

[5] Javeed, M. A., Kumar, M. V., Narendra, H. "Studies on Mix Design of Sustainable Geo-Polymer Concrete", [pdf] International Journal of Innovative Research in Engineering & Management (IJIREM), 2(4), pp. 9–14, 2015. Available at: https://ijirem.org/DOC/3-studies-on-mix-design-of-sustainable.pdf

[6] Bernal, S. A., Rodríguez, E. D., de Gutiérrez, R. M., Gordillo, M., Provis, J. L. "Mechanical and thermal characterisation of geopolymers based on silicate-activated metakaolin/slag blends", Journal of Materials Science, 46, pp. 5477–5486, 2011. https://doi.org/10.1007/s10853-011-5490-z

[7] Davidovits, J. "Geopolymers and geopolymeric materials", Journal of Thermal Analysis, 35, pp. 429–441, 1989. https://doi.org/10.1007/BF01904446

[8] Duxson, P., Provis, J. L., Lukey, G. C., van Deventer, J. S. J. "The role of inorganic polymer technology in the development of 'green concrete'", Cement and Concrete Research, 37, pp. 1590–1597, 2007. https://doi.org/10.1016/j.cemconres.2007.08.018

[9] Hasar, U. C., Eren, N. A., Ozturk, H., Izginli, M., Korkmaz, H., Cevik, A., Nis, A., Irshidat, M. R. "Mechanical and Electromagnetic Properties of Self-Compacted Geopolymer Concretes with NanoSilica and Steel Fiber Additives", IEEE Transactions on Instrumentation and Measurement, 71, 8003508, 2022., https://doi.org/10.1109/TIM.2022.3173272

[10] Eren, N. A., Alzeebaree, R., Çevik, A., Niş, A., Mohammedameen, A., Gülşan, M. E. "The Effects of Recycled Tire Rubbers and Steel Fibers on the Performance of Self-compacting Alkali Activated Concrete", Periodica Polytechnica Civil Engineering, 65(3), pp. 890–900, 2021. https://doi.org/10.3311/PPci.17601

[11] Nguyen-Minh, L., Rovňák, M., Tran-Quoc, T., Nguyenkim, K. "Punching Shear Resistance of Steel Fiber Reinforced Concrete Flat Slabs", Procedia Engineering, 14, pp. 1830–1837, 2011. https://doi.org/10.1016/j.proeng.2011.07.230

[12] Chalah, L., Talah, A. "Permeability of High-Performance Fiber Reinforced Concrete Immersed in High Concentration Sodium Chloride Solution", Periodica Polytechnica Civil Engineering, 66(2), pp. 541–552, 2022. https://doi.org/10.3311/PPci.19632

[13] Marar, K., Eren, Ö., Çelik, T. "Relationship between impact energy and compression toughness energy of high-strength fiber-reinforced concrete", Materials Letters, 47, pp. 297–304, 2001. https://doi.org/10.1016/S0167-577X(00)00253-6

[14] Khan, M. Z. N., Hao, Y., Hao H., Shaikh, F. U. A. "Mechanical properties of ambient cured high strength hybrid steel and synthetic fibers reinforced geopolymer composites", Cement and Concrete Composites, 85, pp. 133–52, 2018. https://doi.org/10.1016/j.cemconcomp.2017.10.011

[15] Eren, N. A., Alzeebaree, R., Çevik, A., Niş, A., Mohammedameen, A., Gülşan, M. E. "Fresh and hardened state performance of self-compacting slag based alkali activated concrete using nanosilica and steel fiber", Journal of Composite Materials, 55(28), pp. 4125–4139, 2021. https://doi.org/10.1177/00219983211032390

[16] Topçu, I. B., Avcular, N. "Collision behaviours of rubberized concrete", Cement and Concrete Research, 27(2), pp. 1893–1898, 1997. https://doi.org/10.1016/S0008-8846(97)00204-4

[17] Reda Taha, M. M., El-Dieb, A. S., Abd El-Wahab, M. A., Abdel-Hameed, M. E. "Mechanical, fracture, and microstructural investigations of rubber concrete", Journal of Materials in Civil Engineering, 20(10), pp. 640–649, 2008. https://doi.org/10.1061/(ASCE)0899-1561(2008)20:10(640)

[18] Al-Tayeb, M. M., Abu Bakar, B. H., Akil, H. M., Ismail, H. "Performance of rubberized and hybrid rubberized concrete structures under static and impact load conditions", Experimental Mechanics, 53(3), pp. 377–384, 2013. https://doi.org/10.1007/s11340-012-9651-z

[19] Liu, F., Zheng, W., Li, L., Feng, W., Ning, G. "Mechanical and fatigue performance of rubber concrete", Construction and Building Materials, 47, pp. 711–719, 2013. https://doi.org/10.1016/j.conbuildmat.2013.05.055

[20] Sukontasukkul, P. "Use of crumb rubber to improve thermal and sound properties of pre-cast concrete panel", Construction and Building Materials, 23(2), pp. 1084–1092, 2009. https://doi.org/10.1016/j.conbuildmat.2008.05.021

[21] Niş, A., Eren, N. A., Çevik, A. "Effects of recycled tyre rubber and steel fibre on the impact resistance of slag-based self-compacting alkali-activated concrete", European Journal of Environmental and Civil Engineering, 27(1), pp. 519–537, 2023. https://doi.org/10.1080/19648189.2022.2052967

[22] Niş, A., Eren, N. A., Çevik, A. "Effects of Nanosilica and Steel Fibers on the Impact Resistance of Slag based Self-Compacting Alkali-Activated Concrete", Ceramics International, 47(7), pp. 23905–23918, 2021. https://doi.org/10.1016/j.ceramint.2021.05.099

[23] Eren, N. A. "Punching shear behavior of geopolymer concrete two-way flat slabs incorporating a combination of nano silica and steel fibers", Construction and Building Materials, 346, 128351, 2022. https://doi.org/10.1016/j.conbuildmat.2022.128351

[24] Eren, N. A. "Behavior of geopolymer concrete under impact", PhD Thesis, Gaziantep University, 2021.

[25] Abdul Aleem, M. I., Arumairaj, P. D. "Optimum mix for the geopolymer concrete", [pdf] Indian Journal of Science and Technology, 5(3), pp. 2299–2301, 2012. Available at: https://www.researchgate.net/profile/Abdul-Aleem/publication/293435150_Optimum_mix_for_the_geopolymer_concrete/links/56ea8d7708ae3a5b48ce51aa/Optimum-mix-for-the-geopolymer-concrete.pdf

[26] Memon, F. A., Nuruddin, M. F., Khan, S., Shafiq, N., Ayub, T. "Effect of sodium hydroxide concentration on fresh properties and compressive strength of self-compacting geopolymer concrete", [pdf] Journal of Engineering Science and Technology, 8(1), pp. 44–56, 2013. Available at: https://jestec.taylors.edu.my/Vol%208%20Issue%201%20February%2013/Vol_8_1_044056_FAREED%20AHMED%20MEMON.pdf

[27] Olivia, M., Nikraz, H. "Properties of fly ash geopolymer concrete designed by Taguchi method", Materials and Design, 36, pp. 191–198, 2012. https://doi.org/10.1016/j.matdes.2011.10.036

[28] Ibrahim, K. I. M., Al-Tersawy, S. H. "The Hybrid Effect of Micro and Nano Silica on the Properties of Normal and High Strength Concrete", IOSR Journal of Mechanical and Civil Engineering (IOSR-JMCE), 14(4), pp. 62–72, 2017. https://doi.org/10.9790/1684-1404066272

[29] Fattuhi, N. I., Clark, L. A. "Cement-based materials containing shredded scrap truck tire rubber", Construction and Building Materials, 10(4), pp. 229–236, 1996.
https://doi.org/10.1016/0950-0618(96)00004-9

[30] Najim, K. B., Hall, M. R. "A review of the fresh/hardened properties and applications for plain- (PRC) and self-compacting rubberized concrete (SCRC)", Construction and Building Materials, 24(11), pp. 2043–2051, 2010.
https://doi.org/10.1016/j.conbuildmat.2010.04.056

[31] Noaman, A. T., Abu Bakar, B. H., Akil, H. M. "Investigation on the Mechanical Properties of Rubberized Steel Fiber Concrete", Engineering Structures and Technologies, 9(2), pp. 79–92, 2017.
https://doi.org/10.3846/2029882X.2017.1309301

[32] Xie, J., Guo, Y., Liu, L., Xie, Z. "Compressive and flexural behaviours of a new steel-fibre-reinforced recycled aggregate concrete with crumb rubber", Construction and Building Materials, 79, pp. 263–272, 2015.
https://doi.org/10.1016/j.conbuildmat.2015.01.036

[33] Elsayed, M., Tayeh, B. A., Mohamed, M., Elymany, M., Mansi, A. H. "Punching shear behaviour of RC flat slabs incorporating recycled coarse aggregates and crumb rubber", Journal of Building Engineering, 44, 103363, 2021.
https://doi.org/10.1016/j.jobe.2021.103363

[34] Gülşan, M. E., Alzeebaree, R., Rasheed, A. A., Niş, A., Kurtoğlu, A. E. "Development of fly ash/slag based self-compacting geopolymer concrete using nano-silica and steel fiber", Construction and Building Materials, 211, pp. 271–283, 2019.
https://doi.org/10.1016/j.conbuildmat.2019.03.228

[35] Nis, A., Özyurt, N., Özturan, T. "Variation of Flexural Performance Parameters Depending on Specimen Size and Fiber Properties", Journal of Materials in Civil Engineering, 32(4), 4020054, 2020.
https://doi.org/10.1061/(ASCE)MT.1943-5533.0003105

[36] Elsayed, M., Tayeh, B. A., Kamal, D. "Effect of crumb rubber on the punching shear behaviour of reinforced concrete slabs with openings", Construction and Building Materials, 311, 125345, 2021.
https://doi.org/10.1016/j.conbuildmat.2021.125345

[37] Hosseini, S.-A., Nematzadeh, M., Chastre, C. "Prediction of shear behavior of steel fiber-reinforced rubberized concrete beams reinforced with glass fiber-reinforced polymer (GFRP) bars", Composite Structures, 256, 113010, 2021.
https://doi.org/10.1016/j.compstruct.2020.113010

[38] Youssf, O., ElGawady, M. A., Mills, J. E. "Experimental investigation of crumb rubber concrete columns under seismic loading", Structures, Elsevier, 3, pp. 13–27, 2015.
https://doi.org/10.1016/j.istruc.2015.02.005

[39] Wardhono, A., Gunasekara, C., Law, D. W., Setunge, S. "Comparison of long term performance between alkali activated slag and fly ash geopolymer concretes", Construction and Building Materials, 143, pp. 272–279, 2017.
https://doi.org/10.1016/j.conbuildmat.2017.03.153

[40] Lee, N. K., Jang, J. G., Lee, H. K. "Shrinkage characteristics of alkali-activated fly ash/slag paste and mortar at early ages", Cement and Concrete Composites, 53, pp. 239–248, 2014.
https://doi.org/10.1016/j.cemconcomp.2014.07.007